Structure and Dynamics of the Cd^{2+} Ion in Aqueous Solution: Ab Initio QM/MM Molecular Dynamics Simulation

Chinapong Kritayakornupong, Kristof Plankensteiner, and Bernd M. Rode*

Department of Theoretical Chemistry, Institute of General, Inorganic and Theoretical Chemistry, University of Innsbruck, A-6020 Innsbruck, Austria

Received: May 26, 2003; In Final Form: September 2, 2003

A hybrid ab initio quantum mechanical/molecular mechanical (QM/MM) molecular dynamics simulation has been performed to evaluate hydration structure and dynamics of the Cd^{2+} ion in aqueous solution. Two hydration shells were identified at the mean distances of 2.3 and 4.8 Å, with coordination numbers of 6 and ~12, respectively, which is in good agreement with X-ray data. Librational and vibrational spectra of the hydrated Cd^{2+} ion have been evaluated, showing a fairly complex spectrum for Cd−O vibrations, whose stretching force constant of 68 N m^{-1} is slightly higher than that for Hg−O vibrations. The mean residence time for the 2nd shell ligands was determined as 10 ps, and the calculated hydration energy of −458 kcal/mol is close to the experimental value of −438 kcal/mol.

1. Introduction

The hydration of the Cd^{2+} ion is an interesting subject for understanding its chemistry, biochemistry, and toxicology.[1−3] The hydration structure of Cd^{2+} has, therefore, been the subject of numerous X-ray diffraction studies[4−9] and an octahedral Cd-$(H_2O)_6^{2+}$ hydrate was identified in dilute $Cd(ClO_4)_2$ solution.[5] Hydration numbers of 3 to 6 were observed in cadmium bromide,[5] chloride,[6] phosphate,[7] sulfate,[5,8] and nitrate[9] solutions of varying concentrations, where anions can occupy sites in the first coordination shell. These results indicate that the composition of the first hydration shell of Cd^{2+} is strongly influenced by counterions thus leading to interpretation problems.[10,11]

Computer simulations such as molecular dynamics (MD) and Monte Carlo (MC) are a powerful tool for evaluating structural and dynamics data for ions in aqueous solution. Classical simulations based on pair interaction potentials have been shown in many cases not to be accurate enough for these studies, even if 3-body corrections are applied.[12−15]

Combined ab initio quantum mechanics/molecular mechanics (QM/MM) methods can solve this problem and have thus been successfully used for evaluating structural and dynamical properties of numerous ions in solution.[16−25] In QM/MM simulations, the system is divided into two regions. The chemically most relevant region, e.g. the interactions between all particles in the first hydration shell, is treated by ab initio quantum mechanics at the Hartree−Fock level, whereas for the rest of the system molecular mechanics with ab initio generated two plus three body potentials are employed.

In the present work, a classical and a QM/MM molecular dynamics simulation at the Hartree−Fock level have been performed for a system consisting of one Cd^{2+} ion plus 499 water molecules. Properties of the hydrated ion have been evaluated in terms of radial distribution functions, coordination numbers, angular distributions, librational and vibrational ligand motions, mean ligand residence time, and hydration energy.

* To whom correspondence should be addressed. E-mail: bernd.m.rode@uibk.ac.at. Phone: +43(0)512/507-5161. Fax: +43(0)512/507-2714.

2. Details of the Calculations

2.1. Pair and Three-Body Potentials. The $Cd^{2+}-H_2O$ pair potentials have been constructed from the ab initio HF-SCF energy surface, using the Los Alamos effective core potential (ECP) plus DZ basis set[26] for Cd^{2+} and Dunning's DZP basis set[27,28] for oxygen and hydrogen atoms. A total of 3061 pair interaction energy points covering distances up to 12 Å and all angular orientations of the ligand were fitted with the Levenberg−Marquardt algorithm to the following analytical formula:

$$\Delta E_{Cd^{2+}-H_2O} = \sum_{ij}\left(\frac{A_{ij}}{r_{ij}^{\ a}} + \frac{B_{ij}}{r_{ij}^{\ b}} + \frac{C_{ij}}{r_{ij}^{\ c}} + \frac{D_{ij}}{r_{ij}^{\ d}} + \frac{q_i q_j}{r_{ij}}\right) \quad (1)$$

A_{ij}, B_{ij}, C_{ij}, and D_{ij} are fitting parameters, r_{ij} is the distance between the ith atom of H_2O and Cd^{2+}, and q_i and q_j are the atomic net charges. All SCF calculations were performed at the RHF level with use of the TURBOMOLE[29−31] program. The final optimized parameters are listed in Table 1.

The three-body energies for $H_2O-Cd^{2+}-H_2O$ were generated by varying both $Cd^{2+}-O$ distances ($1.8 \le r_{Cd^{2+}-O} \le 6.0$ Å), the $O-Cd^{2+}-O$ angle ($60° \le \theta \le 180°$), and the torsional angle ($\tau = 0°$, 45°, and 90°) between planes of water molecules. The three-body corrections for 9085 energy surface points were fitted to the function

$$\Delta E_{3bd} = A_1 \exp(A_2 r_{Cd-O_1}) \exp(A_2 r_{Cd-O_2}) \exp(-A_3 r_{O_1-O_2}) \times [(CL - r_{Cd-O_1})^2 (CL - r_{Cd-O_2})^2] \quad (2)$$

with A_1, A_2, and A_3 being fitting parameters, O_i referring to the center of mass of the water molecules, and CL representing the cutoff limit set to 6.0 Å where the three-body contributions become negligible. The fitting parameters of the three-body correction function are also listed in Table 1.

The molecular dynamics simulation was carried out for the system consisting of one Cd^{2+} plus 499 water molecules in a cubic periodic box with a box length of 24.7 Å at 298.16 K in a canonical NVT ensemble, which was realized by coupling to

10.1021/jp0354548 CCC: $25.00 © 2003 American Chemical Society
Published on Web 11/08/2003

TABLE 1: Final Optimized Parameters of the Analytical Pair Potential Functions and Three-Body Correction Function

pair	A	B	C	D
$Cd^{2+}-O$	−17 829.090 557 5 Å^5	43 822.466 291 8 Å^6	−40 464.540 928 7 Å^8	31 124.264 710 7 Å^{12}
$Cd^{2+}-H$	1 356.945 676 0 Å^4	−6 277.733 351 7 Å^5	8 685.523 224 5 Å^6	

3-body	A_1, kcal mol^{-1} Å4	A_2, Å^{-1}	A_3, Å^{-1}
$H_2O-Cd^{2+}-H_2O$	0.118 992 8	−0.163 556 8	0.549 809 7

[a] Charges on O and H, taken from the BJH−CF2 water−water interaction potential, are −0.6598 and 0.3299, respectively.

TABLE 2: Characteristic Values of the Radial Distribution Functions $g_{\alpha\beta}(r)$ for Cd^{2+} in Water, Determined by Different Molecular Simulation Methods and Experiments[a]

solute	ion/water ratio or molarity (M)	r_{M1}	r_{m1}	n_1	r_{M2}	r_{m2}	n_2	method	ref
Cd^{2+}	1 M	2.29		6				XD	4
$Cd(ClO_4)_2$	2.1 M	2.31		6				XD	5
$Cd(ClO_4)_2$	2.4 M	2.29		6				XD	5
$CdCl_2$	1.26 M	2.37		4				XD	6
$Cd(H_2PO_4)_2$	1 M	2.30		5.1	4.33			XD	7
$CdSO_4$	2 M	2.32		5.2	4.36		11.9	XD	8
$Cd(NO_3)_2$	4.54 M	2.27		5.7				XD	9
Cd^{2+}	1/499	2.27	3.01	8.9	4.50	5.70	23.3	two-body MD	this work
Cd^{2+}	1/499	2.35	3.02	6.0	4.93	5.29	12.2	three-body MD	this work
Cd^{2+}	1/499	2.33	2.78	6.0	4.84	5.27	11.7	QM/MM MD	this work

[a] r_{M1}, r_{M2} and r_{m1}, r_{m2} are the distances of the first and second maximum and the first and second minimum of $g_{\alpha\beta}(r)$ in Å. n_1 and n_2 are the average coordination numbers of the first and second hydration shell, respectively.

an external temperature bath. The density was assumed to be the same as that of pure water (0.997 g cm^{-3}). For Coulombic interactions, a radial cutoff limit was set to half the box length, and it was set to 5 Å and 3 Å for non-Coulombic O−H and H−H interactions, respectively. A reaction field[32] was applied to account for long-range interactions. Interactions between water molecules in the MM region were described by the flexible Bopp−Janscó−Heinzinger central-force water model (BJH-CF2),[33,34] which allows explicit hydrogen movements and thus gives access to the intramolecular vibrations of H_2O also outside the QM region. Our QM/MM simulation protocol ensures a smooth transition of water molecules between the QM region, where all water molecules are fully flexible, and the MM region, where the flexibility is maintained through the BJH-CF2 model. The time step was set to 0.2 fs with respect to the hydrogen motion.

A classical molecular dynamics simulation using pair potentials was performed starting from a random configuration followed by the classical three-body corrected simulation with 100 000 time steps for reequilibration and a further 900 000 time steps (180 ps) for sampling. Finally, the QM/MM molecular dynamics simulation was performed at the Hartree−Fock level, using the same basis sets as in the potential construction. A diameter of 8.0 Å was chosen for the QM region, which still includes a small part of the second hydration shell according to the classical simulation, i.e., at least 6, sometimes 1−2 more ligands. To allow a continuous transition of forces for the exchange of water molecules at the boundary between the QM and the MM region, a smoothing function[35] was applied within an interval of 0.2 Å. A total of 20 000 time steps were needed for reequilibration, and a further 80 000 time steps (16 ps) were collected for data sampling.

The frequencies of vibrational and librational motions of water molecules were calculated from the velocity autocorrelation functions (VACFs) by using normal-coordinate analysis as reported previously.[36,37] The velocities of hydrogen atoms were projected onto the unit vector parallel to the corresponding O−H bond, perpendicular to the O−H bond in the water plane, and perpendicular to the water plane. The six scalar quantities Q_1, Q_2, Q_3, R_1, R_2, and R_3 were defined to describe the symmetric stretching vibration, bending vibration, asymmetric stretching vibration, and rotations around the *x*, *y*, and *z* axes of the water molecules, respectively. All frequencies of water molecules in the first hydration shell, obtained from the QM/MM molecular dynamics simulation, were multiplied by the standard scaling factor of 0.89 to compensate the rather constant systematic error of quantum mechanical frequency calculations at the Hartree−Fock level.[38]

3. Results and Discussion

3.1. Structural Properties. The comparison of structural data obtained by the different molecular dynamics simulation methods and experiments is shown in Table 2. The overestimated average coordination number of 8.9 is a typical result of classical simulations based on pair potential functions. The inclusion of three-body corrections produced $Cd^{2+}-O$ peaks located at 2.35 and 4.93 Å for the first and second hydration shell, respectively, and the corresponding coordination numbers of 6 and 12.2 for first and second hydration shell.

The $Cd^{2+}-O$ and $Cd^{2+}-H$ radial distribution functions (RDF) and their corresponding integration numbers, obtained from the QM/MM molecular dynamics simulation, are depicted in Figure 1. The first sharp peak in the $Cd^{2+}-O$ RDF, corresponding to the first hydration shell, is centered at 2.33 Å, and the second shell peaks at 4.84 Å. The hydration shells are well separated from each other. In experiments,[4−9] the mean $Cd^{2+}-O$ distance for the first hydration shell was reported in the range of 2.18−2.37 Å, depending on the concentration and the type of salt in the solution. The $Cd^{2+}-O$ distance for the first hydration shell, obtained from our QM/MM molecular dynamics simulation, is in good agreement with the octahedral structure of $Cd(H_2O)_6^{2+}$ evaluated by X-ray diffraction for perchlorate solutions,[4,5] where the counterion effect should be small. The distance for the second hydration shell is about 10% larger than the experimental data for hydrogen phosphate[7] and sulfate[8] solutions. The $Cd^{2+}-H$ RDF peaks for the first and second hydration shell are centered at 3.03 and 4.85 Å, respectively, indicating

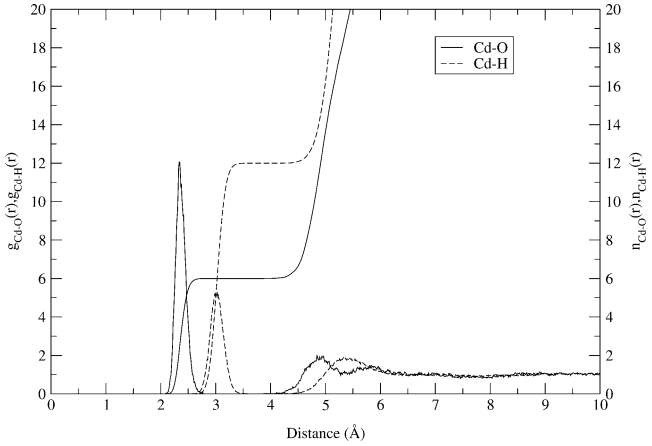

Figure 1. $Cd^{2+}-O$ and $Cd^{2+}-H$ radial distribution functions and their integrations, obtained from the QM/MM molecular dynamics simulation.

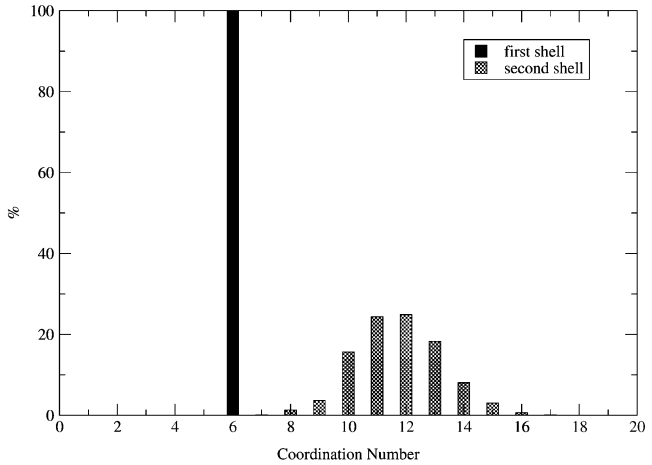

Figure 2. First and second shell coordination number distributions of hydrated Cd^{2+}, obtained from the QM/MM molecular dynamics simulation.

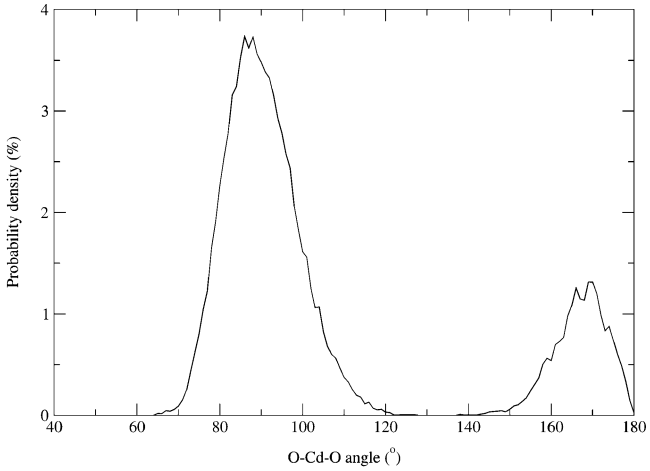

Figure 3. Distribution of the bond angles $O-Cd^{2+}-O$ for the first hydration shell, obtained by QM/MM molecular dynamics simulation.

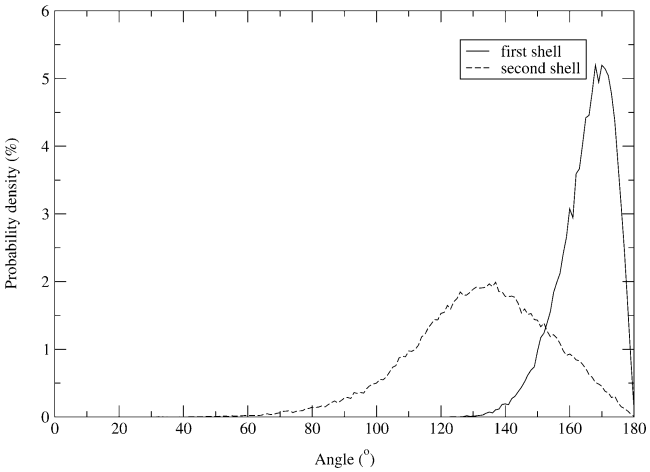

Figure 4. First and second hydration shell distributions of the angle θ, defined by the $Cd^{2+}-O$ axis and the dipole vector of water molecules, obtained by QM/MM molecular dynamics simulation.

domination of ion−dipole interactions for the orientation of water in both hydration shells.

The distribution of coordination numbers of the hydrated Cd^{2+} ion in the first and second hydration shell, obtained from the QM/MM molecular dynamics simulation, has been evaluated and is illustrated in Figure 2. Only coordination number 6 is found for the first hydration shell, while in the second hydration shell the coordination numbers are distributed over a wide range from 8 to 16. The average value of 11.7 is very similar to that of 12.2 (at 4.93 Å) delivered by the classical 3-body corrected molecular dynamics simulation.

The $O-Cd^{2+}-O$ angular distribution for the first hydration shell is presented in Figure 3. It displays two peaks with maximum values at 86° and 169°, corresponding to the octahedral structure of $Cd(H_2O)_6^{2+}$. The angle θ defined by the Cd−O bond axis and the dipole vector of water molecules has been evaluated for observing the ligand orientation around Cd^{2+} in the first and second hydration shell. The classical 3-body corrected molecular dynamics simulation gives the distribution of the angle θ with peaks at 171° and 137° for the first and second hydration shell, which are almost the same as the values of 170° and 137°, obtained from the QM/MM molecular dynamics simulation, shown in Figure 4.

3.2. Dynamical Properties. *3.2.1. Librational Ligand Motions.* Figure 5 displays the power spectra of the VACFs for the librational motions R_x, R_y, and R_z, obtained from the QM/MM molecular dynamics simulation. The frequencies corresponding to the librational motions are compared with frequencies obtained from the inclusion of three-body corrections in Table 3. The frequencies of all rotational modes for the bulk are consistent with those obtained in previous simulations.[37,39,40] A red-shift of the R_y mode is observed for the second hydration shell, whereas the frequencies of the R_x and R_z modes are all blue-shifted, and the amounts of these shifts for the second hydration shell are distinctly higher than those for the hydrated Hg^{2+} ion.[40] The frequency of the R_z mode is shifted to a lower value (44 cm^{-1}) for the first hydration shell: for Hg^{2+} this shift amounts to 28 cm^{-1}. The frequencies of the R_x and R_y modes in the first hydration shell are blue-shifted by 135 and 80 cm^{-1}, respectively. These shifts are smaller than those observed for Hg^{2+} (184 cm^{-1} for R_x and 142 cm^{-1} for R_y mode).[40]

3.2.2. Vibrational Ligand Motions. The vibrational frequencies from the power spectra of the VACFs for the bending mode (Q_2), and the symmetric Q_1 and asymmetric Q_3 stretching modes are shown in Figure 5, and the frequencies are summarized in Table 3. In the classical simulation, Q_2 frequencies of bulk and both hydration shells are not distinguished within methodical accuracy, while Q_1 and Q_3 are slightly red-shifted. In contrast to that, first-shell Q_2 is red-shifted in the QM/MM molecular dynamics simulation, but first-shell Q_1 and Q_3 are blue-shifted by ∼100 and ∼70 cm^{-1}. The same effects have been found for

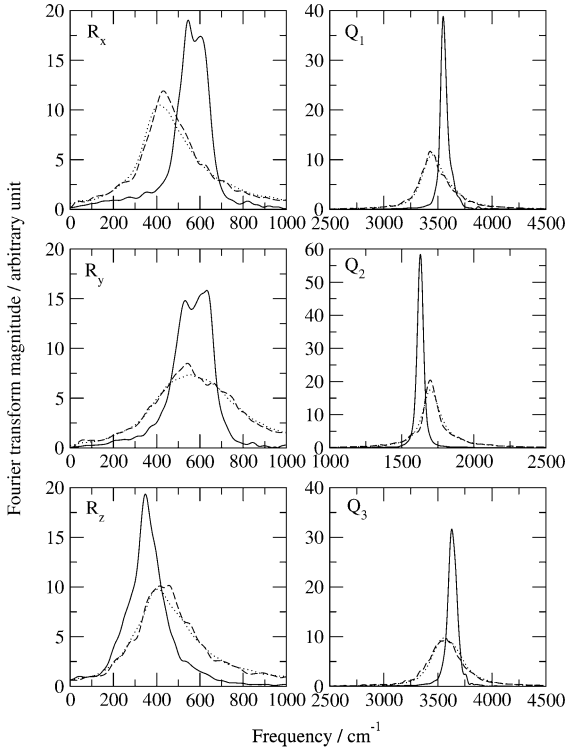

Figure 5. Power spectra of rotational modes R_x, R_y, and R_z, and vibrational modes Q_1, Q_2, and Q_3 of water molecules in the first (solid line), the second (dashed line) hydration shell, and the bulk (dotted line), obtained from the QM/MM molecular dynamics simulation.

TABLE 3: Librational and Vibrational Frequencies of Water Molecules in the First and Second Hydration Shell of the Cd^{2+} Ion and in the Bulk

		frequency[a] (cm^{-1})					
location	method	R_x	R_y	R_z	Q_2	Q_1	Q_3
first shell	classical MD	606	729	360	1690	3121	3258
	QM/MM-MD	**545**	**632**	**348**	**1629**	**3550**	**3629**
second shell	classical MD	468	549	434	1696	3466	3547
	QM/MM-MD[b]	**430**	**542**	**456**	**1697**	**3428**	**3577**
bulk	classical MD	420	591	404	1705	3468	3581
	QM/MM-MD[b]	**410**	**552**	**404**	**1698**	**3450**	**3562**
	classical MD[36]				1715	3475	3580
	classical MD[44]	410	595	405	1705	3475	3595
	liquid-phase exp[45]				**1645**	**3345**	**3455**
	gas-phase exp[46]				1595	3657	3756

[a] R_x, R_y, and R_z denote the librational frequencies of rotation around the three principal axes of the water molecules. Q_1, Q_2, and Q_3 denote the frequencies of symmetric stretching, bending, and asymmetric stretching vibrations of the water molecules, respectively. [b] MM region of this work.

Hg^{2+},[40] but to a smaller extent. While similar red-shifts are obtained for Q_2 in the classical simulations of Cd^{2+} in water, the blue-shifts for Q_1 and Q_3 are not reproduced by the classical simulations, which predict shifts in the opposite direction. It is believed, therefore, that the neutral polarization and charge-transfer effects included in the quantum mechanical treatment play a significant role for the Q_1 and Q_3 vibrations.

3.2.3. Cd^{2+}−O Vibrations. Figure 6 presents the power spectra of the VACFs of the Cd^{2+}−O vibrational modes A_{1g}, E_g, T_{2g}, and T_{1u}, obtained from the QM/MM molecular dynamics simulation. The peak with the highest intensity of the A_{1g} mode is centered at 282 cm^{-1}. Split peaks for the E_g mode are observed at 123, 193, and 267 cm^{-1}. The maximum value of the T_{2g} mode is located at 89 cm^{-1} with an additional smaller peak at 234 cm^{-1}. The T_{1u} spectrum is separated into two peaks

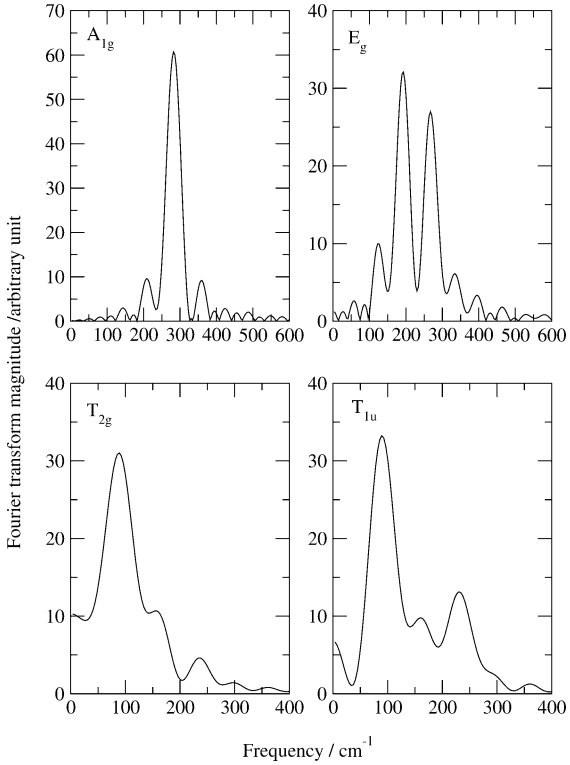

Figure 6. Power spectra of Cd^{2+}−O vibrational modes A_{1g}, E_g, T_{2g}, and T_{1u}, obtained from the QM/MM molecular dynamics simulation.

at 89 and 230 cm^{-1}. The force constant evaluated for the stretching mode is 68 N m^{-1}, which is slightly stronger than the one obtained for Hg^{2+} (64 N m^{-1}).[40] The classical simulation leads to a value of 75 N m^{-1}, which appears clearly overrated.

3.2.4. Water Exchange in the Second Hydration Shell. The reactivity of hydrated ions depends on the dynamics of the water exchange processes between the hydration shells. The expected mean residence time (τ_{res}) for the first hydration shell of the Cd^{2+} ion is in the range of 10^{-8}−10^{-9} s,[41] which explains that no first-shell ligand exchange processes could be observed in our QM/MM simulation. The mean residence time (τ_{res}) of 10 ps for the water molecules in the second hydration shell was determined following the formula introduced by Impey et al.[42] with $\tau^*_{res} = 2$ ps. The mean residence time of 10 ps for Cd^{2+} is nearly the same as that found for Hg^{2+} (13 ps)[40] and is almost two times shorter than that for Co^{2+} (26 ps)[25] and Mn^{2+} (24 ps).[25] The classical simulation produces a τ value of 11 ps, showing that in the case of Cd^{2+} the QM-determined structure of the first hydration shell does not have a significant influence on the MM-treated second hydration shell.

3.2.5. Hydration Energy. Calculated hydration energies from simulations allow a good comparison with experiments. Experimental hydration enthalpies are usually calculated by using the tetraphenylarsonium and tetraphenylborate (TATB) extra-thermodynamic assumption.[43] The thus determined value was −438 kcal/mol, which is in good agreement with our QM/MM simulation value for the hydration energy of −458 kcal/mol. The corresponding value from the classical simulation (−511 kcal/mol) certainly overestimates the ion's stabilization in water.

4. Conclusion

Our results show once more that classical molecular dynamics simulations with three-body corrections are adequate for evaluating structural data but not accurate enough for describing all properties. While the 2nd shell ligand mean residence time is

well reproduced, ion−ligand vibrations and hydration energy are overestimated and require quantum mechanical corrections. Compared to other divalent ions, including Hg^{2+}, these corrections are somewhat smaller for Cd^{2+}, but still appear necessary.

Acknowledgment. Financial support by the Austrian Science Foundation, project No. P16221, and a scholarship from the Austrian Federal Ministry for Foreign Affairs for C.K. are gratefully acknowledged.

References and Notes

(1) Burgess, J. *Metal Ions in Solution*; John Wiley & Sons Ltd.: Chichester, UK, 1978.
(2) Clapham, D. E. *Cell* **1995**, *80*, 259.
(3) Chazin, W. J. *Nat. Struct. Biol.* **1995**, *2*, 707.
(4) Bol, W.; Gerrits, G. J. A.; van Panthaleon van Eck, C. L. *Appl. Crystallogr.* **1970**, *3*, 486.
(5) Ohtaki, H.; Radnai, T. *Chem. Rev.* **1993**, *93*, 1157.
(6) Caminiti, R.; Licheri, G.; Piccaluga, G.; Pinna, G. *Z. Naturforsch.* **1980**, *A35*, 1361.
(7) Caminiti, R. *J. Chem. Phys.* **1982**, *77*, 5682.
(8) Caminiti, R. *Z. Naturforsch.* **1981**, *A36*, 1062.
(9) Caminiti, R.; Cucca, P.; Radnai, T. *J. Phys. Chem.* **1984**, *88*, 2382.
(10) Marcus, Y. *Pure Appl. Chem.* **1987**, *59*, 1093.
(11) Howell, I.; Neilson, G. W. *J. Phys.: Condens. Matter* **1996**, *8*, 4455.
(12) Kritayakornupong, C.; Yagüe, J. I.; Rode, B. M. *J. Phys. Chem. A* **2002**, *106*, 10584.
(13) Corongiu, G.; Clementi, E. *J. Chem. Phys.* **1978**, *69*, 4885.
(14) Texler, N. R.; Rode, B. M. *J. Phys. Chem.* **1995**, *99*, 15714.
(15) Marini, G. W.; Texler, N. R.; Rode, B. M. *J. Phys. Chem.* **1996**, *100*, 6808.
(16) Kerdcharoen, T.; Liedl, K. R.; Rode, B. M. *Chem. Phys.* **1996**, *221*, 313.
(17) Tongraar, A.; Liedl, K. R.; Rode, B. M. *J. Phys. Chem. A* **1997**, *101*, 6299.
(18) Tongraar, A.; Liedl, K. R.; Rode, B. M. *Chem. Phys. Lett.* **1998**, *286*, 56.
(19) Tongraar, A.; Liedl, K. R.; Rode, B. M. *J. Phys. Chem. A* **1998**, *102*, 10340.
(20) Tongraar, A.; Liedl, K. R.; Rode, B. M. *J. Phys. Chem. A* **1999**, *103*, 8524.
(21) Yagüe, J. I.; Mohammed, A. M.; Loeffler, H. H.; Rode, B. M. *J. Phys. Chem. A* **2001**, *105*, 7646.
(22) Schwenk, C. F.; Loeffler, H. H.; Rode, B. M. *J. Chem. Phys.* **2001**, *115*, 10808.
(23) Tongraar, A.; Rode, B. M. *Phys. Chem. Chem. Phys.* **2003**, *5*, 357.
(24) Kritayakornupong, C.; Rode, B. M. *J. Chem. Phys.* **2003**, *118*, 5065.
(25) Rode, B. M.; Schwenk, C. F.; Tongraar, A. *J. Mol. Liquids.* Accepted for publication.
(26) Hay, P. J.; Wadt, W. R. *J. Chem. Phys.* **1985**, *82*, 270.
(27) Dunning, T. H., Jr. *J. Chem. Phys.* **1989**, *90*, 1007.
(28) Dunning, T. H., Jr.; Hay, P. J. *Modern Theoretical Chemistry: Methods of Electronic Structure Theory*; Schaefer, H. F., III, Ed.; Plenum Press: New York, 1977; Vol. 3.
(29) Ahlrichs, R.; Bär, M.; Horn, H.; Häser, M.; Kölmel, C. *Chem. Phys. Lett.* **1989**, *162*, 165.
(30) Ahlrichs, R.; von Arnim, M. *Methods and Techniques in Computational Chemistry: METECC-95*; Cagliari, Sardinia, 1995.
(31) von Arnim, M.; Ahlrichs, R. *J. Comput. Chem.* **1998**, *19*, 1746.
(32) Adams, D. J.; Adams, E. H.; Hills, G. J. *Mol. Phys.* **1979**, *38*, 387.
(33) Stillinger, F. H.; Rahman, A. *J. Chem. Phys.* **1978**, *68*, 666.
(34) Bopp, P.; Janscó, G.; Heinzinger, K. *Chem. Phys. Lett.* **1983**, *98*, 129.
(35) Brooks, B. R.; Bruccoleri, R. E.; Olafson, B. D.; States, D. J.; Swaminathan, S.; Karplus, M. *J. Comput. Chem.* **1983**, *4*, 187.
(36) Bopp, P. *Chem. Phys.* **1986**, *106*, 205.
(37) Inada, Y.; Loeffler, H. H.; Rode, B. M. *Chem. Phys. Lett.* **2002**, *358*, 449.
(38) Grev, R. S.; Janssen, C. L.; Schaefer, H. F., III *J. Chem. Phys.* **1991**, *95*, 5128.
(39) Remsungnen, T.; Rode, B. M. *Chem. Phys. Lett.* **2003**, *367*, 586.
(40) Kritayakornupong, C.; Plankensteiner, K.; Rode, B. M. *Chem. Phys. Lett.* **2003**, *371*, 438.
(41) Helm, L.; Merbach, A. E. *Coord. Chem. Rev.* **1999**, *187*, 151.
(42) Impey, R. W.; Madden, P. A.; McDonald, I. R. *J. Phys. Chem.* **1983**, *87*, 5071.
(43) Marcus, Y. *J. Chem. Soc., Faraday. Trans.* **1987**, *83*, 339.
(44) Spohr, E.; Pálinkás, G.; Heinzinger, K.; Bopp, P.; Probst, M. M. *J. Phys. Chem.* **1988**, *92*, 6754.
(45) Murphy, W. F.; Bernstein, H. J. *J. Phys. Chem.* **1972**, *76*, 1147.
(46) Eisenberg, D.; Kauzmann, W. *The Structure and Properties of Water*; Oxford University Press: Oxford, UK, 1969.